Int. J. Electrochem. Sci., 11 **(2016)** 7811 – 7829, doi: 10.20964/2016.09.25

International Journal of ELECTROCHEMICAL SCIENCE
www.electrochemsci.org

Olive Leaf Extract as a Corrosion Inhibitor of Carbon Steel in CO_2-Saturated Chloride–Carbonate Solution

Gordana Pustaj[1,*], *Frankica Kapor*[1], *Želimir Veinović*[2]

[1] Department of Chemistry, Faculty of Mining Geology and Petroleum Engineering, Zagreb, Croatia
[2] Mining and Geotechnical Engineering Department, Faculty of Mining Geology and Petroleum Engineering, Zagreb, Croatia
[*]E-mail: gordana.pustaj@rgn.hr

Received: 2 May 2016 / *Accepted:* 24 May 2016 / *Published:* 7 August 2016

In the present study corrosion inhibition of carbon steel in CO_2-saturated chloride–carbonate solution by the olive leaf extract has been researched. For that purpose the electrochemical and spectrophotometric techniques such as potentiodynamic polarization, electrochemical impedance spectroscopy and Fourier transform infrared spectroscopy were employed. Both electrochemical techniques, potentiodynamic polarization and electrochemical impedance spectroscopy, demonstrate that olive leaf extract inhibits the carbon steel corrosion in CO_2-saturated chloride–carbonate solution. It was determined that the inhibition efficiency increases with increasing concentration of the olive leaf extract. The olive leaf extract achieves high corrosion efficiency as a mixed type inhibitor, with a prevailing influence on the anode process. Recorded electrochemical impedance spectra in the presence of the extract show the presence of the inhibitor film on the steel surface. This is further confirmed by the recording in Fourier transform infrared spectroscopy spectrum.

Keywords: Carbon steel; CO_2 corrosion; Inhibitor

1. INTRODUCTION

Carbon steels are widely used and preferred to others materials in oil and gas industry. The reasons are economic and the fact that the carbon steel corrosion is mostly uniform. One of the most common and aggressive environment found in the petroleum industry is a fluid with high concentration of chlorides containing carbon dioxide [1–4]. CO_2 is naturally occurring component in many oil and gas fields where CO_2 is present in amounts varying from trace levels to as much as 50 % associated with water, oil and gas production. CO_2 may also be purposely added as part of secondary enhanced oil recovery processes [5–7].

Carbon dioxide is soluble in water as follows [8]:

$$CO_2(aq) + H_2O \leftrightarrow H_2CO_3(aq) \quad (1)$$

In an oxygen–free environment, three cathodic reactions and one anodic reaction control the corrosion process [1, 8–10]:

$$2H^+ + 2e^- \rightarrow H_2 \quad (2)$$
$$2H_2CO_3 + 2e^- \rightarrow 2HCO_3^- + H_2 \quad (3)$$
$$2HCO_3^- + 2e^- \rightarrow 2CO_3^{2-} + H_2 \quad (4)$$
$$Fe \rightarrow Fe^{2+} + 2e^- \quad (5)$$

However, the exact mechanism of the cathodic reaction is still being debated. It was recently reported that the dominant cathodic reaction is reduction of hydrogen ions (reaction 2) formed by dissociation of carbonic acid. This mechanism is so called “buffering effect” [11].

This leads to CO_2 corrosion, usually called sweet corrosion [1–4]. In order to solve this problem many corrosion control methods and research are considered in various oilfields around the world. The most economic corrosion protection method of carbon steels is the use of organic inhibitors [7, 12]. Typical corrosion inhibitors are employed in small concentrations.

In CO_2 corrosion protection imidazoline and its derivatives are found to be most effective organic inhibitors and therefore are widely used. [13–15]. Because of their biodegradability, they are also considered as green corrosion inhibitor [13, 16, 17]. They have good adsorption properties and form chemical film on the steel surface that protects it from CO_2 corrosion. However, it was determined that imidazoline aggravate localized corrosion by forming a small number of major anodes, which leads to highly concentrated anodic dissolution [5, 18]. Pitting corrosion still occurred in the presence of chloride in CO_2-saturated solutions containing imidazoline derivatives as corrosion inhibitors [5, 19].

Today, industrial requirements for corrosion inhibitors refer not only to their efficacy (in general and localized corrosion inhibition) but to safety as well. It is necessary for those compounds to meet the additional requirements as non-mutagenic and non-carcinogenic characteristic and need to be more environmentally acceptable than systems currently in use [20–22].

Plant extracts are environmentally acceptable, relatively easily available and renewable source of naturally synthesized chemical compounds that can be extracted with low cost and used as corrosion inhibitor. Many natural products were tested as corrosion inhibitors in different environments [17, 23]. Test results showed that plant extracts could be applied as effective environmentally acceptable corrosion inhibitors [24–45].

In the Mediterranean area, olive leaves are one of the by-products of farming of the olive grove. It can be found in high amounts in the olive oil industries (about 10 % of the total weight of the olives) and as an accumulation during purifying of the olive trees [46, 47]. The major active components in olive leaves are found to be oleuropein and its derivates such as hydroxytyrosol and tyrosol, caffeic acid, p–coumaric acid, vanillic acid, vanillin, luteolin, diosmetin, rutin, luteolin–7–glucoside, apigenin–7–glucoside and diosmetin–7–glucoside [20, 48, 49].

The objective of the present study was to investigate the inhibition properties of olive leaf extract (OLE) and surface processes on carbon steel, labelled J55, in CO_2-saturated chloride–carbonate solution at 35 °C. In the present work potentiodinamic polarization, electrochemical impedance spectroscopy (EIS) and Fourier transform infrared spectroscopy (FTIR) were employed in order to clarify how this inhibitor works.

2. EXPERIMENTAL

2.1. Sample preparation

The chemical composition of the J55 carbon steel employed in this study was determined by optical emission spectrometry on spectrophotometer GDS 850, Leco, and that is (wt.%): 0.35 C, 0.35 Si, 1.09 Mn, 0.007 P, 0.024 S, 0.09 Cr, 0.07 Ni, 0.01 Mo, 0.10 Cu, <0.01 V, Fe balance. The steel has a ferrite–pearlite microstructure, as shown in Fig. 1.

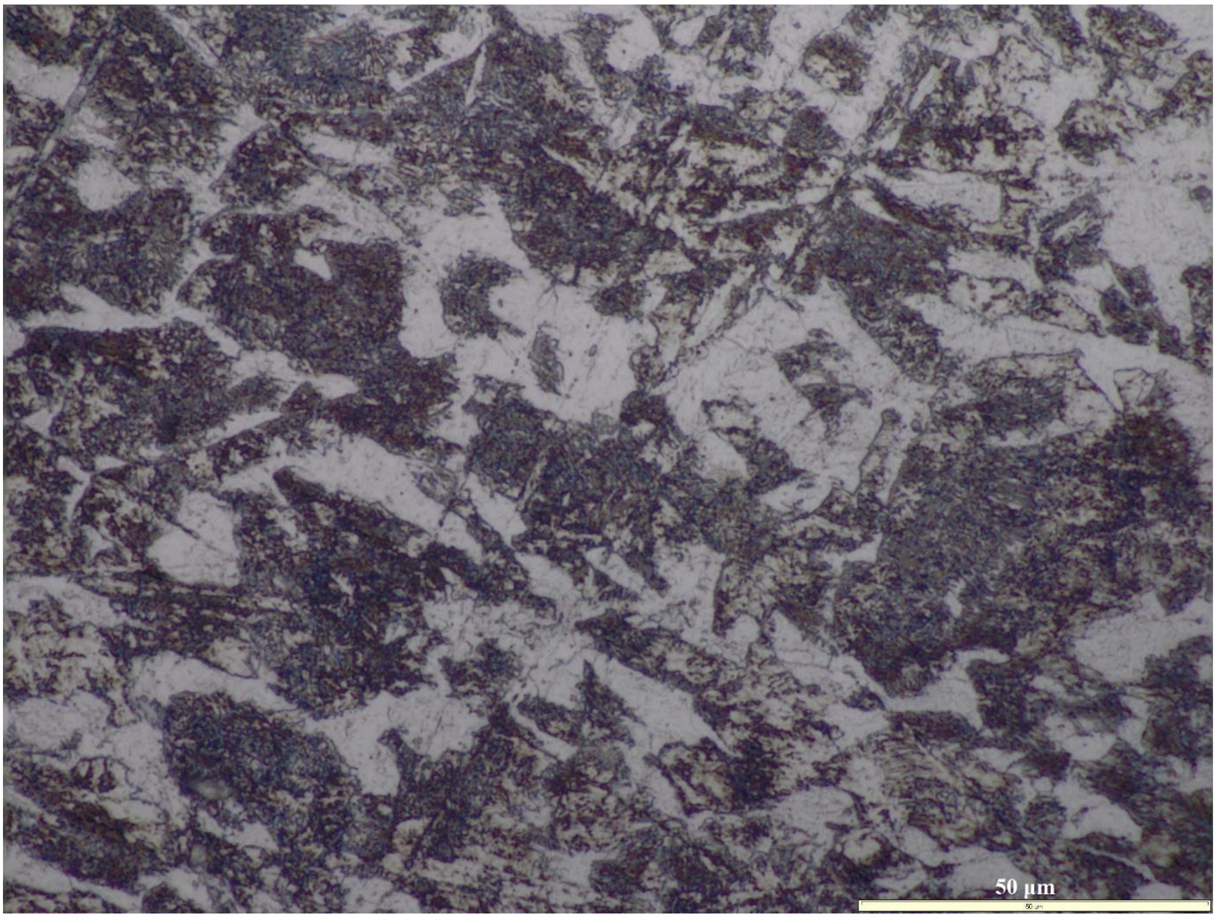

Figure 1. Ferritic-pearlite microstructure of J55 carbon steel recorded with light microscope with magnification 1000 times.

The exposed surface of the electrode was 1 cm^2 and wet ground with silicon carbide abrasive paper up to 1200 grit, rinsed with double distilled water and degreased in 96 % ethanol and dried in an air stream.

2.2. Test solution

The test media were 800 mL of chloride–carbonate solution saturated with CO_2. It was prepared to a concentration of 30 g L^{-1} NaCl, 0.1 g L^{-1} $NaHCO_3$ and 0.1 g L^{-1} $CaCO_3$. All chemicals used for preparing test solution were analytical grade. The solutions were saturated with CO_2 gas bubbling for 1 h prior to test and continuously during the testing (pH = 5). All experiments were performed at temperature 35 ± 1 °C under dynamic conditions (magnetic stirrer, 300 min^{-1}).

Natural, commercially available, olive leaf extract (OLE) powder was used as a corrosion inhibitor. The content of the main active component of the extract, oleuropein, determined by the manufacturer, by HPLC was 20.74%. OLE powder was added at concentrations from 50 to 300 mg L^{-1}. Chemical structure of oleuropein and other active components in OLE are presented in Fig. 2.

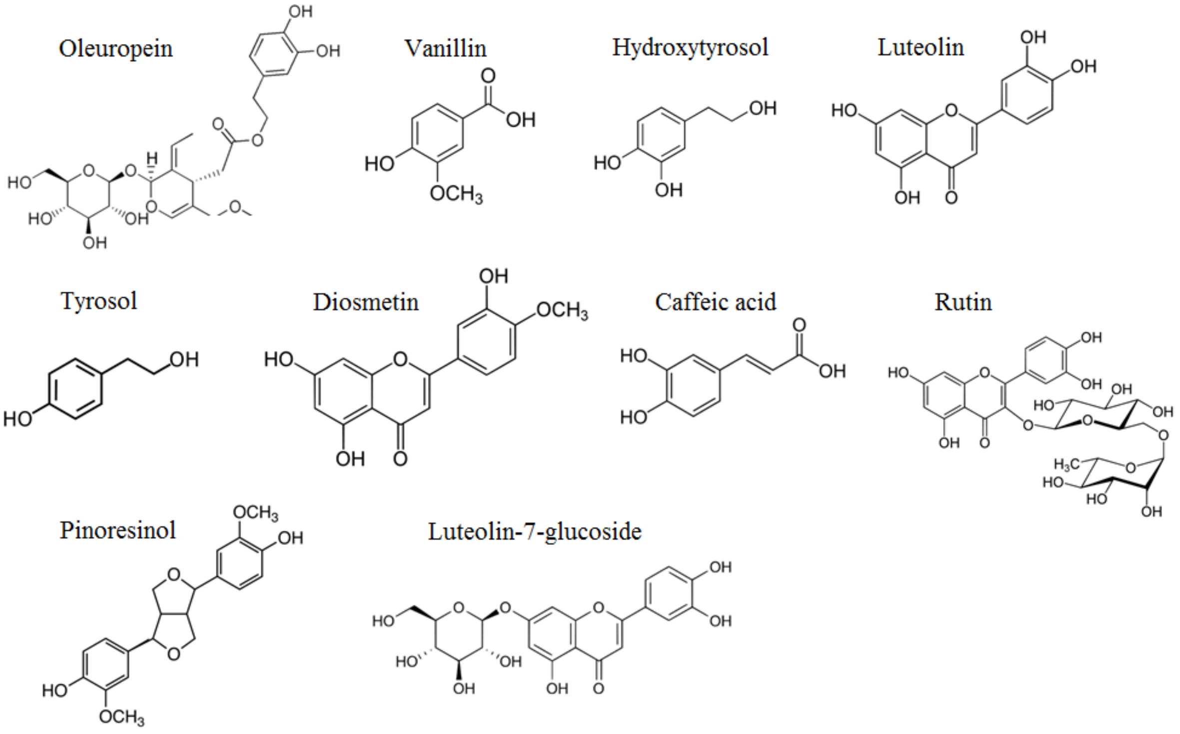

Figure 2. Chemical structure of OLE active components.

2.3. Electrochemical measurements

The electrochemical measurements were carried out using a three–electrode glass cell under atmospheric pressure and temperature 35 °C. The carbon steel J55 was the working electrode, saturated calomel electrode (SCE) was used as a reference electrode, and two graphite rods were used as counter electrodes. All electrochemical measurements were carried out using Potentiostat/Galvanostat, Model EG&G PAR 378 (Great Britain). Prior to electrochemical measurements a stabilization period of 1 h was allowed to attain a stable value of E_{corr} [50].

Tafel curves were obtain by changing the electrode potential automatically from –250 to +250 mV versus corrosion potential, E_{corr}, at a scan rate of 0.1660 mV s^{-1}. Corrosion current densities (j_{corr})

were determinate by extrapolation of the linear Tafel parts of anodic and cathodic curves to corrosion potential. The software Power Suite was used for analysing the results.

EIS measurements were carried out at open circuit potential with amplitude of 5 mV *ac* in the frequency range of 100 kHz to 1 mHz. The tests were performed at E_{corr} after immersion working electrode for 1 h, 2 h, 3 h, 4 h and 24 h in tested solution. The Nyquist representation of the impedance data were analysed with the software ZSimpWin.

For each experiment fresh prepared solution and working electrode were used. To assess the reproducibility, all measurement were carried out three or four times. The relative standard deviation was less than 5 %.

2.4. FTIR characterization

FTIR spectra were recorded in a FTIR Spectrum One, Perkin Elmer spectrophotometer, (Great Britain), which extended from 650 to 4000 cm^{-1}, using the Attenuated Total Reflectance (ATR) technique. The specimen for FTIR characterization was the thin adsorption layer formed on carbon steel J55 surface after immersion for 24 h in CO_2-saturated chloride–carbonate solution containing 300 mg L^{-1} OLE. The sample was tested in its basic form and there was no need for any prior sample preparation for recording. Before FTIR recording of carbon steel sample, the sample was rinsed with distilled water and dried in a nitrogen stream.

3. RESULTS AND DISCUSSION

3.1. Potentiodynamic polarization curves

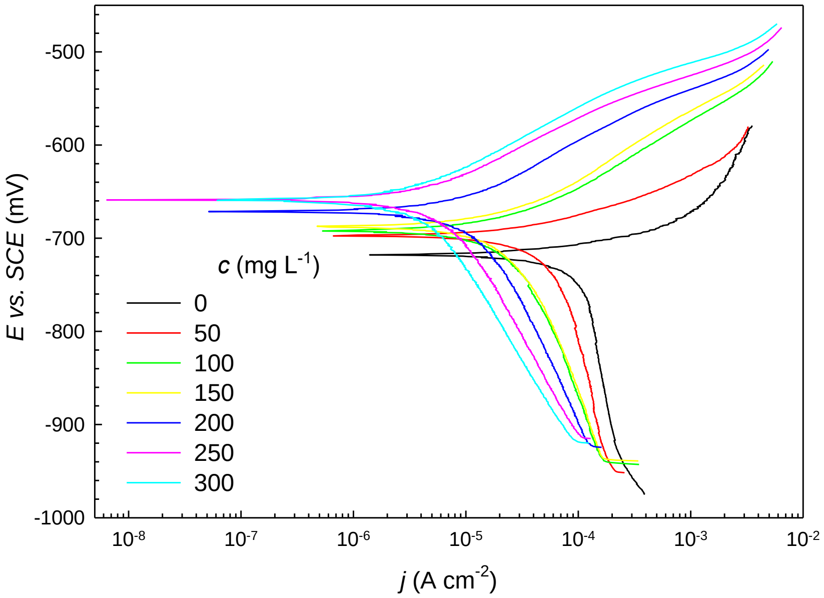

Figure 3. Potentiodynamic polarization curves for J55 carbon steel in CO_2-saturated chloride–carbonate solution in the absence and in the presence of OLE at 35 °C.

Polarization measurements were carried out on freshly abraded samples of J55 carbon steel in CO_2-saturated chloride–carbonate solution in the absence and presence of 50 mg L^{-1}, 100 mg L^{-1}, 150 mg L^{-1}, 200 mg L^{-1}, 250 mg L^{-1} and 300 mg L^{-1} OLE at 35 °C. Figure 3 shows the polarization curves for J55 carbon steel in CO_2-saturated chloride–carbonate solution containing various concentration of OLE.

Table 1. Electrochemical parameters obtained from Tafel extrapolation of potentiodynamic polarization curves for carbon steel J55 in CO_2-saturated chloride–carbonate solution in the absence and in the presence of OLE at 35 °C.

c / mg L^{-1}	E_{corr} / mV	j_{corr} / µA cm^{-2}	$-\beta_c$ / mV dec^{-1}	β_a / mV dec^{-1}	v_{corr} / mm y^{-1}	IE / %
0	-718	107.70	710.19	43.29	1.2500	/
50	-697	51.08	394.59	48.33	0.5927	52.57
100	-689	22.86	272.37	66.46	0.2653	78.77
150	-687	20.27	234.93	74.48	0.2352	81.18
200	-669	10.45	211.82	79.48	0.1213	90.30
250	-659	6.49	211.89	78.40	0.0753	93.97
300	-658	4.56	203.62	74.57	0.0529	95.78

The relevant electrochemical parameters obtained from the polarization curves are presented in Table 1. The inhibition efficiency (*IE*) of the OLE was determined from the following Eq. (6):

$$IE\,(\%) = \frac{j_{corr}^{o} - j_{corr}^{inh}}{j_{corr}^{o}} \times 100 \qquad (6)$$

where j_{corr}^{o} and j_{corr}^{inh} are the corrosion current densities in the absence and presence of OLE as inhibitor, respectively. The current densities (j_{corr}) values were calculated using Tafel extrapolation method. Both Tafel slopes were extrapolated until the lines intersected at E_{corr}.

In the presence of the OLE the shift of the corrosion potential (E_{corr}) to positive direction is observed. This propose that the effect of the OLE on the anodic reaction is more significant in comparison with the effect on the cathodic reaction [7, 13, 49]. This positive shift in the corrosion potential (E_{corr}) is normally observed when applying corrosion inhibitors on mild steel in CO_2 containing brines [51]. From Table 1, it can be seen that with increasing the concentration of the OLE, the corrosion current densities (j_{corr}^{inh}) and corrosion rates (v_{corr}) decreased and the inhibitor efficiency (*IE*) increased. The high *IE* value proposed a complete coverage of the sample with inhibitor molecules. The highest inhibitor efficiency, *IE* = 95.78 %, achieved OLE at maximum concentration at 300 mg L^{-1}. From the results (given in table 1) it can be seen the modification of the anodic and cathodic Tafel slopes values with OLE concentration. There is an influence of the OLE addition on both corrosion reaction: it reduces the anodic dissolution of iron and suppresses the cathodic hydrogen evolution [52–57].

After each polarization measurement, working electrode samples are observed by optical microscopy, whereby a uniform and regular corrosion attacks are noticed. Figures 4a and 4b show J55 carbon steel surface after scanning of the potentiodynamic polarization curves in the absence and presence of OLE, respectively. The carbon steel surface in the presence of the OLE is uniform and smooth, without localized attack, Fig. 4a, unlike the rough surface, covered with corrosion products of uninhibited system, Fig. 4a.

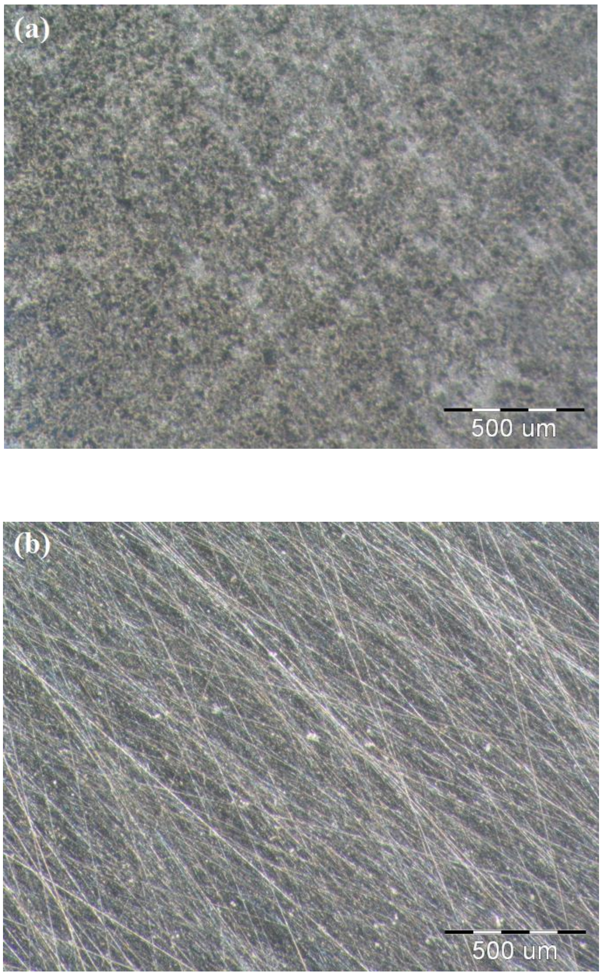

Figure 4. The J55 carbon steel surface after potentiodynamic polarization in CO_2-saturated chloride–carbonate solution (a) in the absence and (b) in the presence of 300 mg L^{-1} OLE at 35 °C (optical microscope, ×6.5)

The results indicated that the OLE acted as a mixed type inhibitor with predominant influence on the anode process [7, 58]. The retardation of carbon steel corrosion processes take place at anodic and cathodic reaction sites and it is attributed to the adsorption of the OLE at the steel surface. The potentiodynamic polarization results revealed that the OLE showed very good inhibitor effectiveness on the studied J55 carbon steel in CO_2-saturated chloride–carbonate solution at 35 °C.

The anodic Tafel slope in the absence of OLE, β_a = 43,29 mV dec^{-1}, is in the accordance with the anodic Tafel slopes 30–60 mV dec^{-1} seen in the literature for similar testing condition [59–62]. In the presence of OLE the anodic Tafel slopes show the slight increase. This could be explained by forming the complex [(FeHO)Inh] in the presence of the OLE [63].

3.2. EIS tests

Electrochemical impedance spectroscopy was carried out to study interfacial changes at the steel surface in the absence and presence of OLE as inhibitor. Figures 5–9 show the Nyquist and Bode plots recorded on the J55 carbon steel in CO_2-saturated chloride–carbonate solution in the absence and presence of OLE. These plots were recorded after 1 h, 2 h, 3 h, 4 h and 24 h of immersion of J55 steel in tested solution.

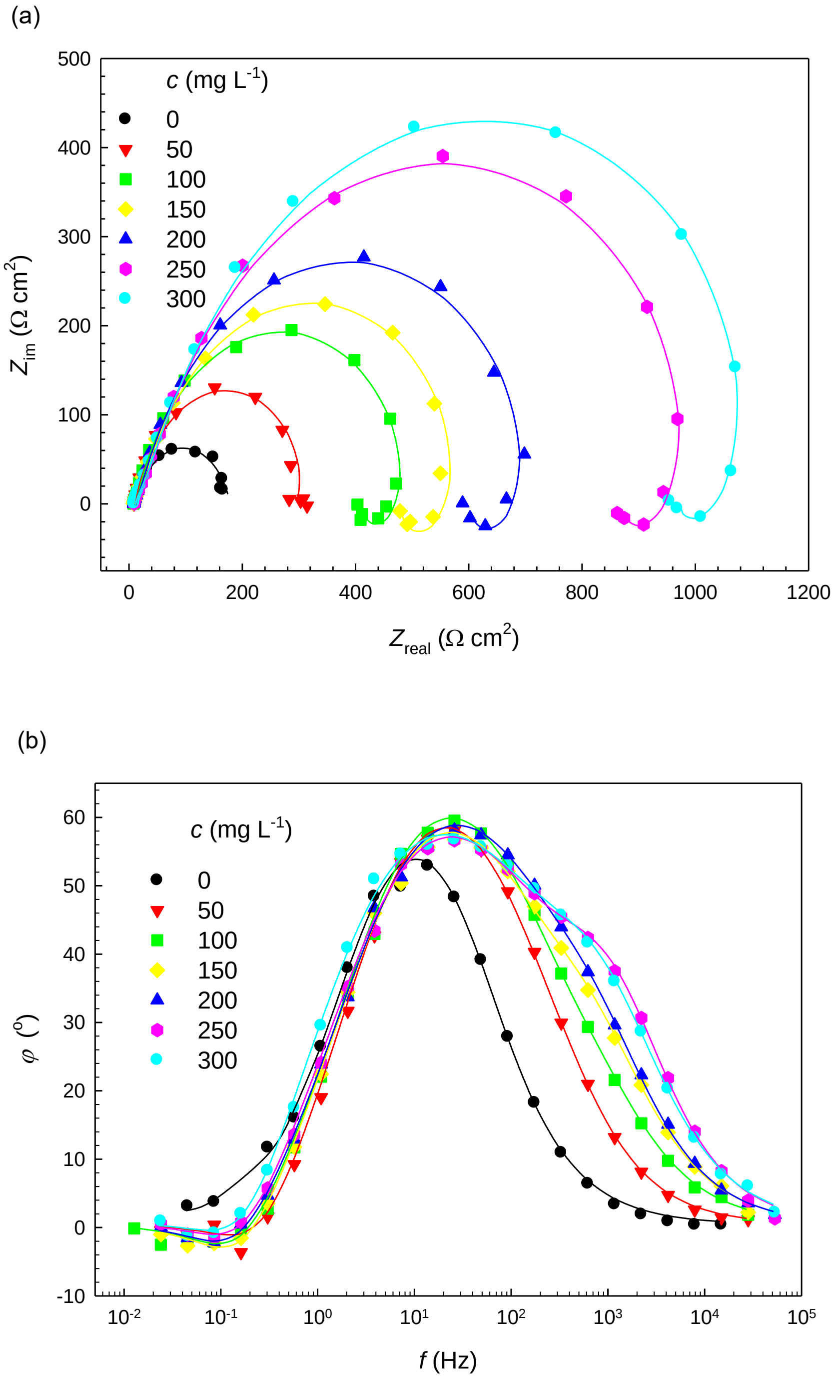

Figure 5. (a) Nyquist and (b) Bode plots for J55 carbon steel in CO_2-saturated chloride–carbonate solution in the absence and in the presence of OLE at 35 °C after 1 h of immersion.

The impedance diagrams recorded in the presence of OLE showed much larger impedance than in its absence and it increases with the inhibitor concentration and exposure time. These results suggest that the addition of OLE promotes the formation of a protective film [64]. The diameter of semicircles increases with the increase of OLE concentration and exposure time.

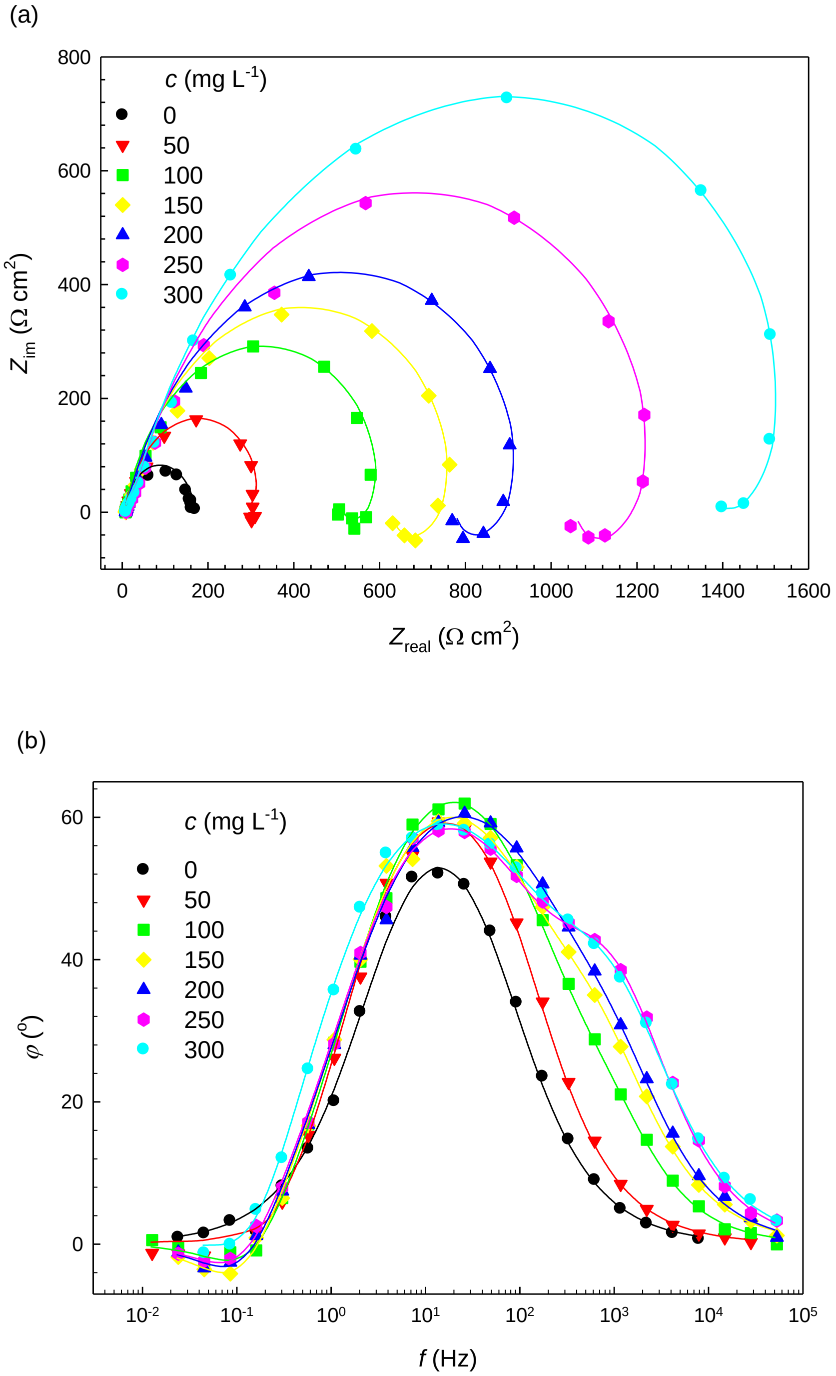

Figure 6. (a) Nyquist and (b) Bode plots for J55 carbon steel in CO_2-saturated chloride–carbonate solution in the absence and in the presence of OLE at 35 °C after 2 h of immersion.

Nyquist diagrams are irregular semicircles. The irregular semicircle shape often indicates the frequency dispersion of interfacial impedance [65–67]. Such phenomenon is usually characteristic of the metal surface inhomogeneity as a result of surface roughness or interfacial phenomena. This is typical for solid metal electrodes [65, 68–70].

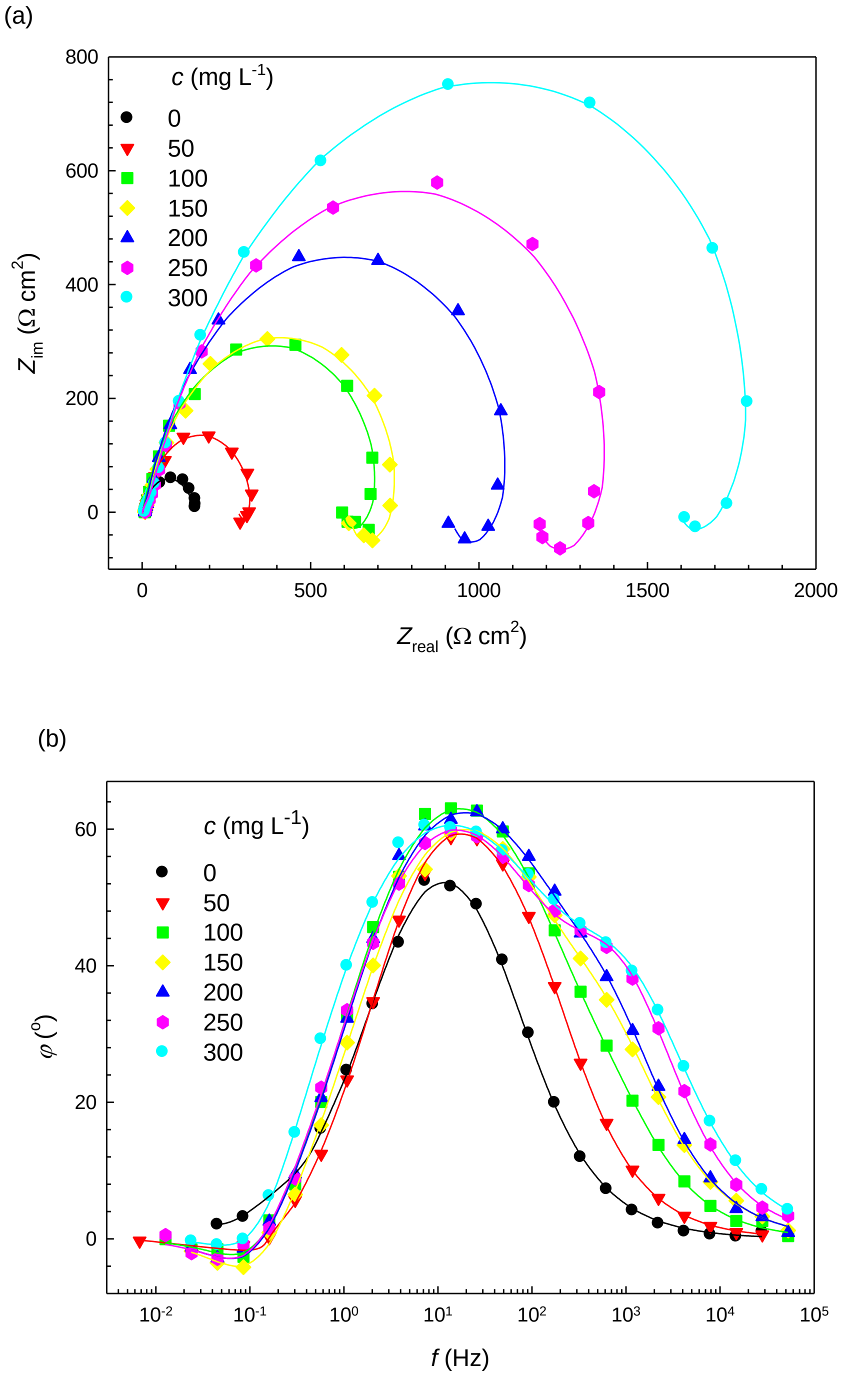

Figure 7. (a) Nyquist and (b) Bode plots for J55 carbon steel in CO_2-saturated chloride–carbonate solution in the absence and in the presence of OLE at 35 °C after 3 h of immersion.

To quantify the EIS electrochemical parameters, equivalent circuits (EC) shown in Fig. 10 are used for fitting EIS data. In the equivalent circuits: R_{el} is the electrolyte resistance, R_{ct} is the charge transfer resistance, CPE_{dl} is the constant phase element which presents the capacitance of double layer,

R_L is the inductance resistance, L is the inductance, CPE_{inh} is the constant phase element which represent the capacitance of inhibitor film, and R_{po} is the resistance of the inhibitor film pores [10].

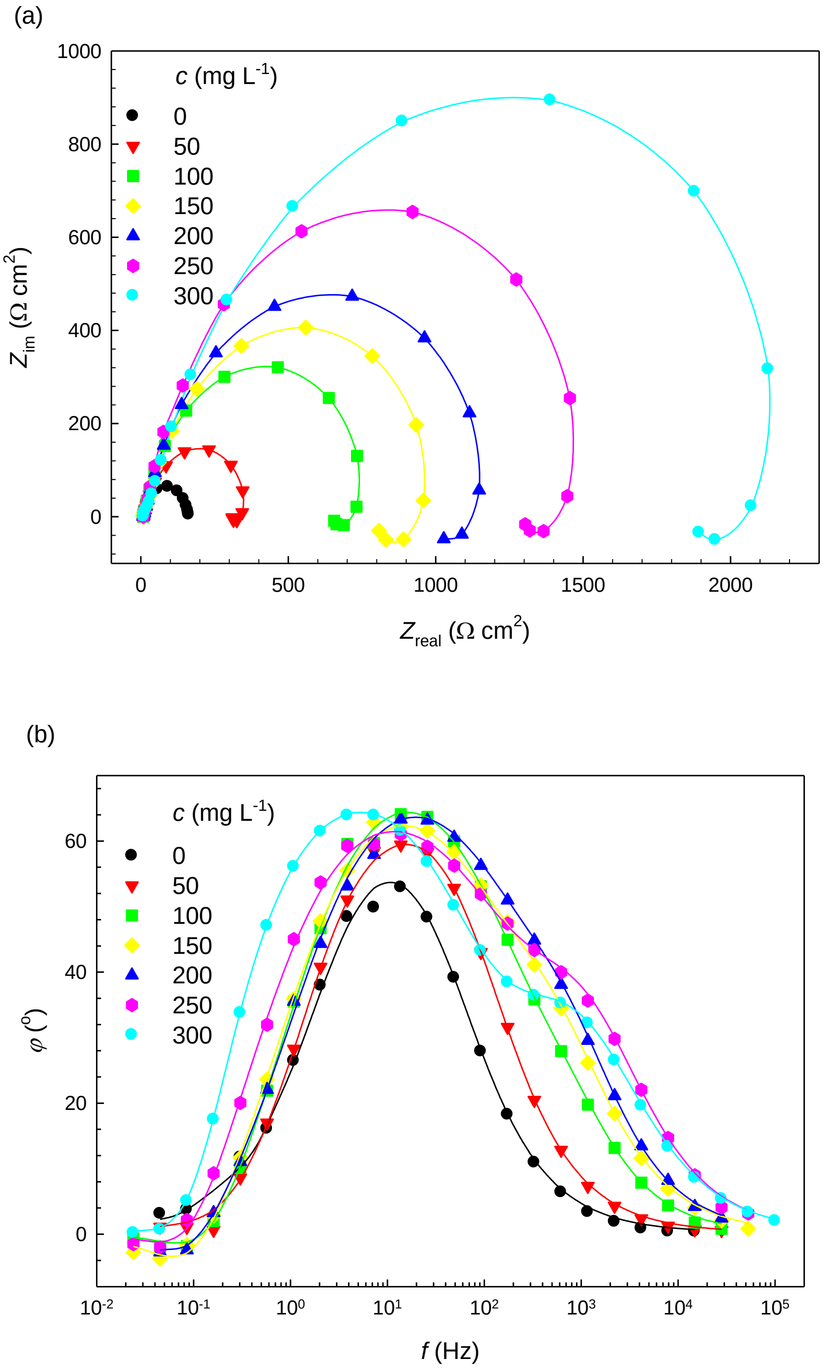

Figure 8. (a) Nyquist and (b) Bode plots for J55 carbon steel in CO_2-saturated chloride–carbonate solution in the absence and in the presence of OLE at 35 °C after 4 h of immersion.

The constant phase elements (CPE) are used to describe the capacitances of double layer and inhibitor film. These element (CPE) takes into account the deviation from the ideal capacitive behaviour due to surface inhomogeneity, roughness and adsorption effects. The impedance of CPE is calculated by the equation [10]:

$$Z_{\mathrm{CPE}} = \frac{1}{Y}(j\omega)^{-n} \tag{7}$$

where Y is a proportional factor, $j = \sqrt{-1}$, $\omega = 2\pi f$, n is the dispersion coefficient associated with surface inhomogeneity. For n = 0, it presents a resistance with $R = Y^{-1}$; for n =1, it presents a capacitance with $C = Y$ [71].

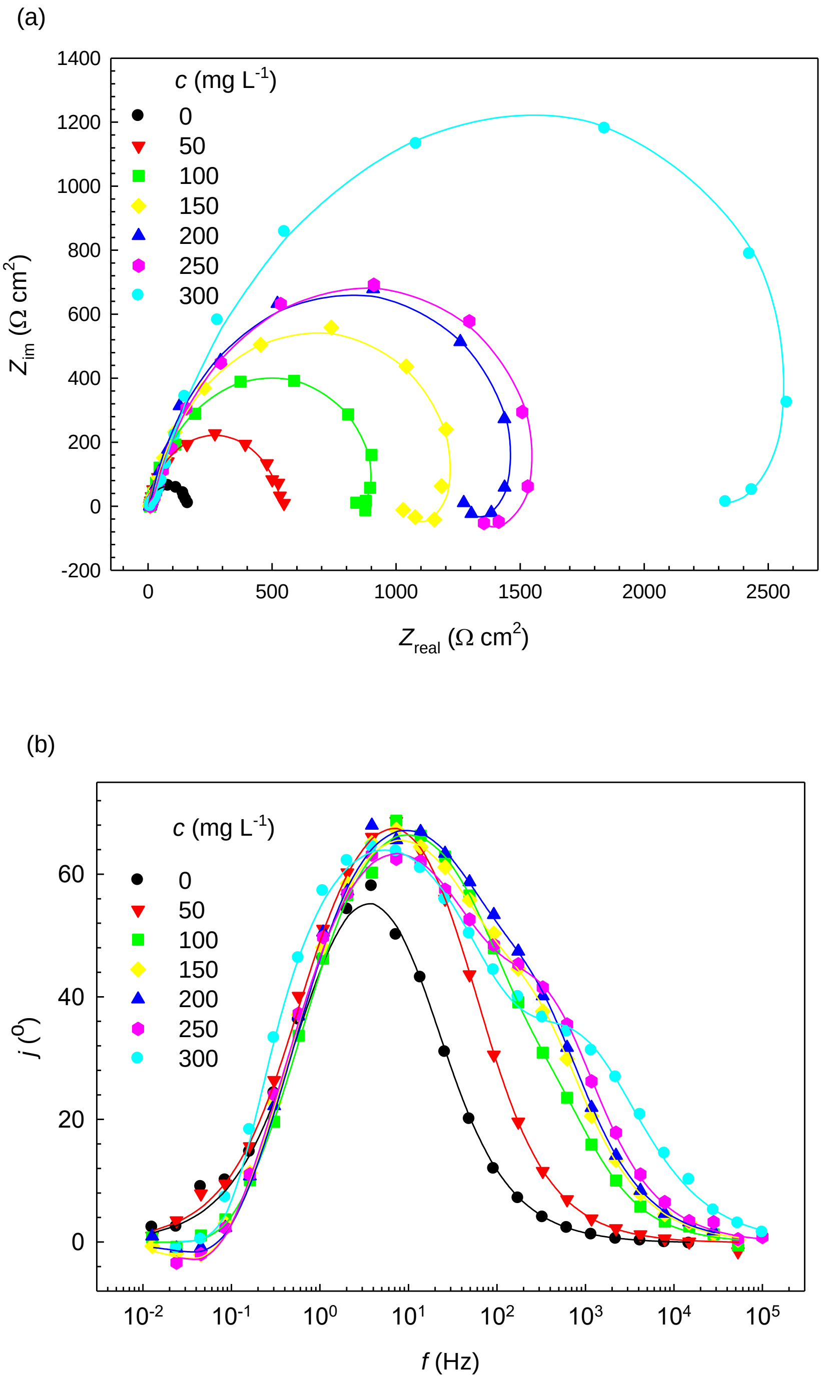

Figure 9. (a) Nyquist and (b) Bode plots for J55 carbon steel in CO_2-saturated chloride–carbonate solution in the absence and in the presence of OLE at 35 °C after 24 h of immersion.

The EC in Fig. 10a is used for fitting the recorded EIS data: in the absence and in the presence of 50 mg L^{-1} of OLE at all tested times and in the presence of 100 mg L^{-1} of OLE after 1 h of E_{corr} stabilisation. The EC in Fig. 10b is used for fitting the EIS data of the remaining inhibited systems (at OLE concentration of 100 mg L^{-1} after 1 h of E_{corr} stabilisation and at concentration of 150–300 mg L^{-1} during all tested periods).

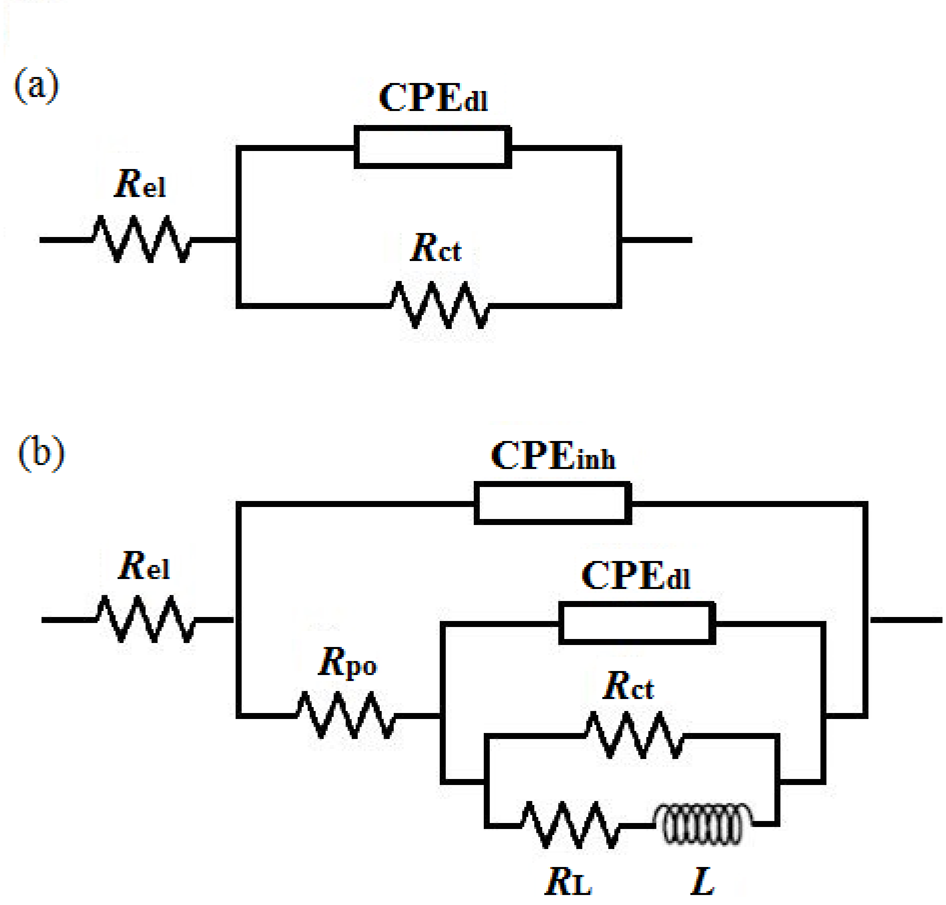

Figure 10. Equivalent circuits used for the modelling of the impedance data.

On the presented impedance spectra (Nyquist and Bode plots), points represent measured while lines represent the fitted results. I can be seen that the fitted and measured results match quite well in both Nyquist and Bode plots. In all cases, the fitted data have an average error lower than 5 %. Table 2 lists the fitted electrochemical parameters. The inhibition efficiency, *IE*, based on the charge transfer resistance, is calculated using the following relation:

$$IE\ (\%) = \frac{R_{\mathrm{ct}}^{\mathrm{inh}} - R_{\mathrm{ct}}^{0}}{R_{\mathrm{ct}}^{\mathrm{inh}}} \times 100 \qquad (8)$$

where $R_{\mathrm{ct}}^{\mathrm{inh}}$ and R_{ct}^{0} are the charge transfer resistances for J55 carbon steel in the presence and absence of inhibitor, respectively.

Nyquist plots, recorded for the system in the absence of the OLE show the existence of single capacitive semicircle. The fitting results show that the proportional factor Y_{dl} of CPE increases with time. This increase in capacitance (Y_{dl}) value for uninhibited system is attributed to an increase in the surface area available for cathodic reaction and precipitation of corrosion products. Surface area increases as a result of preferential dissolution of ferrite while cementite protrudes on the steel surface. This leads to a decrease in the values of R_{ct} with time, Table 2 [10].

Table 2. Electrochemical parameters fitted from the measured EIS data for carbon steel J55 in CO_2-saturated chloride–carbonate solution in the absence and in the presence of OLE at 35 °C.

c (mg L^{-1})	t (h)	Y_{inh} * 10^{-6} (Ω^{-1} cm $^{-2}$ s^n)	n_{inh}	R_{po} (Ω cm^2)	Y_{dl} * 10^{-6} (Ω^{-1} cm $^{-2}$ s^n)	n_{dl}	R_{ct} (Ω cm^2)	*IE* (%)
0	1	-	-	-	575.3	0.8318	172.6	-
	2	-	-	-	578.1	0.8571	157.9	-
	3	-	-	-	716.5	0.8504	155.2	-
	4	-	-	-	740.1	0.8662	155.1	-
	24	-	-	-	1887	0.8848	153.7	-
50	1	-	-	-	385.8	0.8649	309.6	44.25
	2	-	-	-	350.0	0.8568	337.5	53.21
	3	-	-	-	291.6	0.8572	340.6	54.43
	4	-	-	-	306.2	0.8339	374.1	58.54
	24	-	-	-	570.1	0.9001	530.0	71.00
100	1	-	-	-	233.7	0.7990	521.1	66.88
	2	37.99	0.9799	11.43	175.4	0.7970	637.7	75.24
	3	80.99	0.9165	20.75	134.8	0.8301	698.0	77.77
	4	68.09	0.9386	18.35	140.9	0.8169	782.5	80.18
	24	70.23	0.9686	13.68	202.4	0.8316	966.7	84.10
150	1	132.4	0.8730	29.73	71.54	0.7918	585.1	70.50
	2	86.11	0.8452	38.35	85.79	0.8315	768.6	79.46
	3	74.99	0.8616	35.36	96.45	0.8842	770.2	79.85
	4	79.43	0.8760	38.53	104.9	0.8167	1012	84.67
	24	103.7	0.8936	44.28	117.6	0.8653	1285	88.04
200	1	118.7	0.8529	70.24	49.15	0.8004	680.7	74.64
	2	30.23	0.9344	21.32	102.3	0.7533	997.5	84.17
	3	57.55	0.8802	42.57	81.15	0.8097	1135	86.33
	4	40.82	0.9252	31.35	100.9	0.7938	1213	87.21
	24	78.70	0.9144	46.87	96.66	0.8602	1545	90.05
250	1	68.64	0.9052	85.00	61.66	0.7563	1063	83.76
	2	74.99	0.8819	35.36	96.45	0.8009	1262	87.49
	3	26.27	0.9034	45.21	97.12	0.7908	1504	89.68
	4	72.10	0.8809	58.92	107.1	0.8731	1584	90.21
	24	34.17	0.8861	52.16	90.51	0.8070	1617	90.49
300	1	77.61	0.8407	87.85	62.50	0.8023	1074	83.93
	2	42.47	0.8474	56.09	84.76	0.7835	1673	90.56
	3	46.56	0.8350	58.70	80.96	0.8096	1927	91.95
	4	64.75	0.8439	45.77	103.3	0.8014	2461	93.70
	24	60.08	0.8154	65.96	68.57	0.8666	2897	94.69

The Y_{dl} values decreased in the presence of OLE in comparison with the system in the absence of the extract, which indicates the adsorption of the extract at the metal-electrolyte interface. The R_{ct} increases with the OLE concentration and exposure time. The greatest inhibitive effect, *IE* = 94.69 %, is observed at 300 mg L^{-1} of OLE after 24 h of time exposure which presents R_{ct} value of 2897 Ω cm^2. Inhibition efficiencies obtained from potentiodynamic polarization curves and EIS are quite comparable.

A high value of charge transfer resistance is an indicator of slow corrosion process, while decrease in capacitance of the metal, in the presence of inhibitor, suggests better corrosion protection. Double layer capacity is given by Helmholtz's model:

$$C_{\mathrm{dl}} = \frac{\varepsilon\varepsilon_0 A}{d} \tag{9}$$

where d is the thickness of the protective layer, ε is the dielectric constant of the medium, ε_0 is the permittivity of vacuum and A is the effective surface area of the electrode. The decrease of Y_{dl} value i.e., double layer capacity, C_{dl}, is attributed to the lowering of the dielectric constant value due to the replacement of the water molecules with the organic inhibitor molecules (which have lower dielectric constant) at the metal-electrolyte interface. Another explanation could be the increase of the double layer thickness due to the adsorption of larger inhibitory molecules at the metal-electrolyte interface [63, 72–75].

The recorded impedance spectra in the absence and in the presence of the 50 mg L^{-1} of OLE, Figs. 5–9, exhibit one single capacitive loop, which indicates that the corrosion of steel is mainly controlled by a charge transfer process [76, 77]. On the other hand, the impedance spectra recorded for the systems in the presence of 100–300 mg L^{-1} of the OLE consist of two capacitive arcs at high and middle frequencies (better seen in Bode plots) followed by a small inductive loop at low frequencies in the Nyquist plots, Figs. 5–9.

In accordance with the Nyquist plots, three time constants are present in the Bode plots, Figs. 5–9. At inhibitor concentration higher than 200 mg L^{-1} the second time constant can be clear seen Figs. 5–9. Time constants that emerge at high frequencies range can be attribute to the presence of porous inhibitor film [60, 78]. Since the inhibitor film is porous, the electrolyte passes through the pores and corrosion takes place at that surface area. This process is evidenced by the existence of the low frequency time constant [7, 79]. The inductive loop at very low frequencies in Nyquist plots may be attribute to the relaxation process obtained by adsorption of inhibitor species on the electrode surface [80].

The maximum phase angle of the low frequency time constant maintains the constant value, which may be relate to the formation of a protective thin layer, Figs. 5–9. The time constant observed at the high frequency range indicates the existence of a thin isolating and protective inhibitor film formed on the steel surface [7, 81]. This is in the agreement with the increase in the anodic slope noticed on the polarization curves in the presence of the inhibitor, Fig. 3.

3.3. FTIR results

The OLE contain organic compounds, and these organic compounds were adsorbed on the J55 carbon steel surface providing protection against corrosion. FTIR spectra was carried out to identify the adsorbed extract on the carbon steel surface. Figures 11a and 11b show the FTIR ATR spectrum of the powdered OLE and protective film formed on the carbon steel surface after 24 h exposure to the inhibited system at 35 °C, respectively.

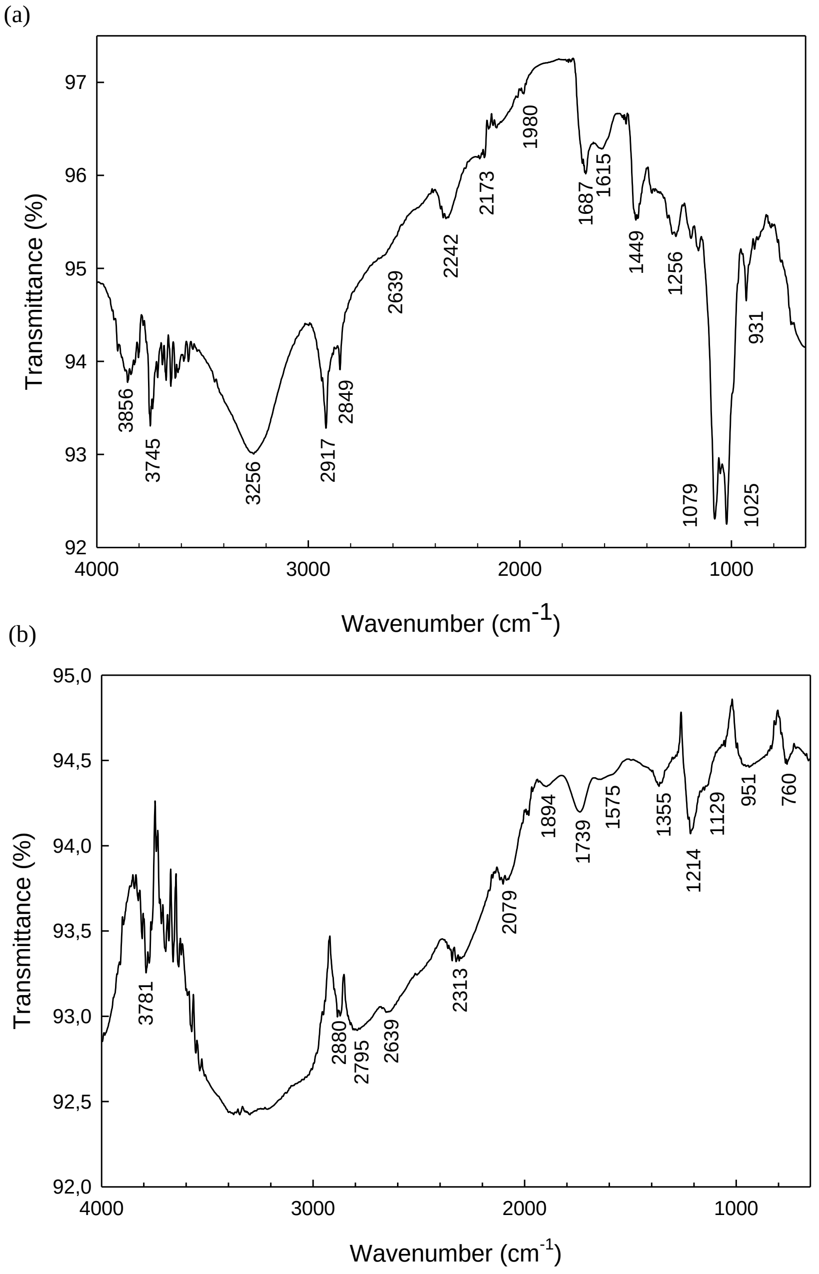

Figure 11. FTIR spectra of (a) OLE powder and (b) surface film formed on J55 carbon steel after 24 h immersion in CO_2-saturated chloride–carbonate solution containing 300 mg L^{-1} OLE at 35 °C.

Peaks observed for the powdered olive leaf extract at 3256 and 1687 cm^{-1} are characteristic of O–H and C=O vibration stretching of O–H and C=O groups, possible of oleuropein and other active compounds present in the olive leaf extract [82–84]. Adsorption bands at 2917 cm^{-1}, 2849 cm^{-1} and 1449 cm^{-1} are related to C–H asymmetric stretching vibration [85]. IR band at 1615 cm^{-1} is attributed to the C=O vibrations in amides. Strong bands at 1079 cm^{-1} and 1025 cm^{-1} are attributable to vibration of C–O ether and ester groups in the compounds of olive leaf extract [84–86].

ATR FTIR spectra of adsorbed protective layer formed on J55 carbon steel surface after 24 h immersion in CO_2 chloride–carbonate solution containing 300 mg L^{-1} of OLE at 35 °C is shown in Fig. 11b. The stretching vibration shifts towards higher wave number values. This could be a result of complexes Fe^{2+}–OLE formation, adsorbed on the steel surface, which is responsible for carbon steel corrosion protection. FTIR spectra of the protective film shows the shift of IR bands due to stretching vibration of C=O and C–O. It is possible that OLE compounds are bonded on the steel surface via free C=O and C–O groups of active components [84].

FTIR results confirm the adsorption of the OLE on the J55 carbon steel surface previously proved via *ac* and *dc* electrochemical measuring techniques.

4. CONCLUSION

OLE has been confirmed as a very good corrosion inhibitor for carbon steel J55 in CO_2-saturated chloride–carbonate solution. The presence of OLE promotes the formation of protective organic compound layer on carbon steel surface. The J55 carbon steel immersed in OLE containing solution exhibited a more positive E_{corr} and lower j_{corr} values than in its absence. Potentiodynamic polarization measurements revealed that OLE inhibits both partial corrosion reaction, with a slightly stronger inhibition of the anodic corrosion reaction. The inhibiton performance increased with increasing OLE concentration and time exposure, confirming the improved corrosion resistance. The charge transfer resistance also increased with an increasing concentration of OLE addition and exposure time. The addition of OLE inhibits general and localized corrosion. The results obtained from two employed methods are in reasonable agreement.

References

1. M. Heydari and M. Javidi, *Corros. Sci.,* 61 (2012) 148
2. D. A. Lopez, S. N. Simison and S. R. de Sanchez, *Corros. Sci*., 47 (2005) 735
3. D. A. Lopez, W. H. Schreiner, S. R. de Sanchez and S. N. Simison, *Appl. Surf. Sci.,* 236 (2004) 77
4. X. Zhang, F. Wang, Y. He and Y. Du, *Corros. Sci.,* 43 (2001) 1417
5. N. D. Nam, Q. V. Bui, M. Mathesh, M. Y. J. Tan and M. Forsyth, *Corros. Sci.,* 76 (2013) 257
6. R. Wan, *Advanced well completion engineering*, Elsevier Inc., Oxford (2011)
7. M. P. Desimone, G. Grundmeier, G. Gordillo and S. N. Simison, Electrochim. Acta, 56 (2011) 2990
8. S. George and S. Nešić, *Corrosion*, 63 (2007) 178
9. S. Nešić, *Uhlig's Corrosion Handbook*), John Wiley & Sons, New Jersey (2011)
10. J. B. Sun, G. A. Zhang, W. Liu and M. X. Lu, *Corros. Sci.,* 57 (2012) 131

11. X. T. Tran, B. Brown and S. Nešić, Proceedings of Corrosion/2015, Paper No. 5671, NACE International, Houston (2015)
12. M. Mobin, S. Zehra and M. Parveen, *J. Mol. Liq.*, 216 (2016) 598
13. H. Zhang, X. Pang, M. Zhou, C. Liu, L. Wei and K. Gao, *Appl. Surf. Sci.,* 356 (2015) 63
14. W. H. Durnie, B. J. Kinsella, R. de Marco and A. Jefferson, *J. Appl. Electrochem.,* 31 (2001) 1221
15. P. C. Okafor, C. B. Liu, X. Liu and Y. G. Zheng, *J. Appl. Electrochem.,* 39 (2009) 2535
16. D. A. López, W. H. Schreiner, S. R. de Sánchez and S. N. Simison, *Appl. Surf. Sci.,* 207 (2003) 69
17. J. G. Gonzalez-Rodriguez, T. Zeferino-Rodriguez, D. M. Ortega, S. Serna, B. Campillo, M. Casales, E. Valenzuela and J. A. Juarez-Islas, *Int. J. Electrochem. Sci.,* 2 (2007) 883
18. Y. J. Tan, *Corros. Sci.,* 53 (2011) 2041
19. X. Liu, P. C. Okafor and Y. G. Zheng, *Corros. Sci.*, 51 (2009) 744
20. A. M. Abdel-Gaber, B. A. Abd-El-Nabey, E. Khamis and D. E. Abd-El-Khalek, *Desalination,* 278 (2011) 337
21. V. V. Paustovskaya, *Prot. Met.,* 36 (2000) 89
22. C. A. Grillo, M. V. Mirífico, M. L. Morales, M. A. Reigosa and M. Fernández Lorenzo de Mele, *J. Hazard. Mater.*, 170 (2009) 1173
23. A.K. Singh, S. Mohapatra and B. Pani, *J. Ind. Eng. Chem*., 2016, DOI:10.1016/j.jiec.2015.10.014
24. R. M. Saleh, A. A. Ismail and A. A. El Hosary, *Brit. Corros J.*, 17 (1982) 131
25. K. Pravinar, A. Hussein, G. Varkey and G. Singh, *Transaction of the SAEST,* 28 (1993) 8
26. A. Y. El-Etre, M. Abdallah and Z. E. El-Tantawy, *Corros. Sci.*, 47 (2005) 385
27. E. E. Oguzie, *Port. Electrochimica Acta,* 26 (2007) 303
28. R. Saratha, S. V. Priya and P. Thilagavathy, *E-J. Chem.,* 6 (2009) 785
29. O. K. Abiola and A. O. James, *Corros. Sci.,* 52 (2010) 661
30. A. K. Satapathy, G. Gunasekaran, S. C. Sahoo, K. Amit and P. V. Rodrigues, *Corros. Sci.,* 51 (2009) 2848.
31. F. S. de Souza and A. Spinelli, *Corros. Sci.,* 51 (2009) 642
32. P. C. Okafor, M. E. Ikpi, I. E. Uwah, E. E. Ebenso, U. J. Ekpe and S. A. Umoren, *Corros. Sci.,* 50 (2008) 2310
33. J. C. da Rocha, J. A. da Cunha Ponciano Gomes and E. D'Elia, *Corros. Sci.,* 52 (2010) 2341
34. L. G. da Trindade and R. S. Gonçalves, *Corros. Sci.*, 51 (2009) 1578
35. E. A. Noor, *J. Appl. Electrochem.,* 39 (2009) 1465
36. F. A. Ayeni, V. S. Aigbodion and S. A. Yaro: *Eurasian Chem. Technol. J.,* 9 (2007) 91
37. E. Khamis and N. Alandis, *Materialwiss. Werkstofftech*., 33 (2002) 550
38. I. B. Obot and N. O. Obi-Egbedi, *Int. J. Electrochem. Sci.,* 4 (2009) 1277
39. A. Y. El-Etre, *J. Colloid Interface Sci.,* 314 (2007) 578
40. R. M. Saleh, Abd El Alim, A. Mahasen and A. A. El Hosary, *Corrosion Prevention and Control,* 30 (1983) 9
41. E. E. Oguzie, C. K. Enenebeaku, C. O. Akalezi, S. C. Okoro, A. A. Ayuk and E. N. Ejike, *J. Colloid Interface Sci.,* 349 (2010) 283
42. S. T. Arab, A. M. Al-Turkustani and R. H. Al-Dhahiri, *J. Korean Chem. Soc.*, 52 (2008) 281
43. S. Rajendran, S. Shanmugapriya, T. Rajalakshmi and A. J. Amal Raj, *Corrosion,* 61 (2005) 685
44. T. Jain, R. Chowdhary, P. Arora and S. P. Mathur, *Bull. Electrochem.*, 21 (2005) 23
45. J. C. da Rocha, J. A. C. Ponciano Gomes, E. D´Elia, A. P. Gil Cruz, L. M. C. Cabral, A. G. Torres and M. V. C. Monteiro, *Int. J. Electrochem. Sci.,* 7 (2012) 11941
46. H. Jemai, M. Bouaziz, I. Fki, A. El Feki and S. Sayadi, *Chem. Biol. Interact.*, 176 (2008) 88
47. J. Tabera, A. Guinda, A. Ruiz-Rodríguez, F. J. Senoráns, E. Ibánez, T. Albi and G. Reglero, *J. Agric. Food Chem.*, 52 (2004) 4774
48. O. H. Lee, B. Y. Lee, J. Lee, H. B. Lee, J. Y. Son, C. S. Park, K. Shetty and Y. C. Kim, *Bioresource Technol.,* 100 (2009) 6107
49. G. Pustaj, F. Kapor and P. Kvasnička, *Int. J. Mater. Res.*, 105 (2014) 992

50. A. Singh, Y. Lin, M. A. Quraishi, L. O. Olasunkanmi, O. E. Fayemi, Y. Sasikumar, B. Ramaganthan, I. Bahadur, I. B. Obot, A. S. Adekunle, M. M. Kabanda and E. E. Ebenso, *Molecules*, 20 (2015) 15122
51. M. Knag, K. Bilkova, E. Gulbrandsen, P. Carlsen and J. Sjoblom, *Corrosion Sci.,* 48 (2006) 2592
52. Z. H. Tao, S. T. Zhang, W. H. Li and B. R. Hou, *Corros. Sci.*, 51 (2009) 2588
53. A. K. Satapathy, G. Gunasekaran, S. C. Sahoo, Kumar Amit and P. V. Rodrigues, *Corros. Sci.,* 51 (2009) 2848
54. E. S. Ferreira, C. Giacomelli, F. C. Giacomelli and A. Spinelli, *Mater. Chem. Phys.*, 83 (2004) 129
55. Y. Yan, W. H. Li, L. K. Cai and B. R. Hou, *Electrochim. Acta,* 53 (2008) 5953
56. W. H. Li, Q. He, S. T. Zhang, C. L. Pei and B. R. Hou, *J. Appl. Electrochem*., 38 (2008) 289
57. V. S. Sastri, *Green Corrosion Inhibitors*, John Wiley & Sons, New Jersey (2011)
58. 28 R L. Li, W. Xu, J. Lei, J. Wang, J. He, N. Li and F. Pan, *RSC Adv*., 2015, DOI:10.1039/C5RA19088F
59. C. de Waard and D. E. Milliams, *Corrosion,* 31 (1975) 177
60. I. Esih, T. Sorić and Z. Pavlinić, *Brit. Corros. J.,* 33 (1998) 309
61. W. Schwenk, *Werkst. Korros.,* 25 (1974) 643
62. G. Schmitt and B. Rothmann, *Werkst. Korros.*, 29 (1978) 98
63. P. C. Okafor, X. Liu and Y. G. Zheng, *Corros. Sci*., 51 (2009) 761
64. N. D. Nam, Q. V. Bui, M. Mathesh, M. Y. J. Tan and M. Forsyth, *Corros. Sci.,* 76 (2013) 257
65. L. J. Li, X. P. Zhang, J. L. Lei, J. X. He, S. T. Zhang and F. S. Pan, *Asian J. Chem.*, 24 (2012) 1649
66. L. Larabi, Y. Harek, M. Traianel and A. Mansri, *Appl. Electrochem.*, 34 (2004) 833
67. F. Mansfeld, M. W. Kendig and S. Tsai, *Corrosion*, 38 (1982) 570
68. H. Shih and F. Mansfeld, *Corros. Sci.,* 29 (1989) 1235
69. S. Martinez and M. Metikoš-Huković, *J. Appl. Electrochem.*, 33 (2003) 1137
70. F. Bentiss, M. Lebrini, H. Vezin, F. Chai, M. Traisnel and M. Lagrené, *Corros. Sci.,* 51 (2009) 2165
71. Y. Lu, H. Jing, Y. Han and L. Xu, *J. Mater. Eng. Perform*., 25 (2016) 565
72. S. Webster, D. Harrop, A. McMahon and G. J. Partidge, *Proceedings of NACE Corrosion/1993.*, Paper No. 109, NACE International, Houston (1993)
73. A. Edwards, C. Osborne, S. Webster, D. Klenerman, M. Joseph, P. Ostovar and M. Doyle, *Corros. Sci.*, 36 (1994) 315
74. K. Videm, *Proceedings of Corrosion/2000,* Paper No. 39, NACE International, Houston (2000)
75. C. Cao. *Corros. Sci.*, 38 (1996) 2073
76. S. Deng and X. Li, *Corros. Sci.*, 55 (2012) 407
77. M. Behpour, S. M. Ghoreishi, N. Mohammadi, N. Soltani and M. Salavati-Niasari, *Corros. Sci.,* 52 (2010) 4046
78. G. Zhang, C. Chen, M. Lu, C. Chai and Y. Wu, *Mater. Chem. Phys.*, 105 (2007) 331
79. L. D. Paolinelli, T. Pérez and S. N. Simison, *Corrosion Sci.*, 50 (2008) 2456
80. A. K. Singh and M. A. Quraishi, *Corros. Sci.,* 52 (2010) 152
81. O. Olivares-Xometl, N. V. Likhanova, M. A. Dominguez-Aguilar, J. M. Hallen, L. S. Zamudio and E. Arce, *Appl. Surf. Sci.,* 252 (2006) 2139
82. M. A. Quraishi, J. Rawat and M. Ajmal, *J. Appl. Electrochem.,* 30 (2000) 745
83. A. Y. El-Etre, *J. Colloid Interface Sci*., 314 (2007) 578
84. M. M. H. Khalil, E. H. Ismail and F. El-Magdoub, *Arab. J. Chem.*, 5 (2012) 431
85. X. H. Li, S. D. Deng, H. Fu and G. N. Mu, *J. Appl. Electrochem*., 39 (2009) 1125
86. M. M. H. Khalil, E. H. Ismail, K. Z. El-Baghdady and D. Mohamed, *Arab. J. Chem.*, 7 (2013) 1131